INSTITUTE OF PLASMA PHYSICS

NAGOYA UNIVERSITY

RESEARCH REPORT

NAGOYA, JAPAN

System of Inner Current Annuli Arranged along the Minor Axis of a Torus

Akihiro Mohri
and
Taijiro Uchida

IPPJ-127 June 1972

Further communication about this report is to be sent to the Research Information Center, Institute of Plasma Physics, Nagoya University, Nagoya, JAPAN.

Synopsis

A magnetic field configuration produced by immersing poloidal current rings in a toroidal magnetic field is examined, covering wide range of parameters: number of the rings, aspect ratio of the ring and amount of the ring current. Owing to the toroidal effect, null-field lines shift from their original positions in case of the linear configuration. An averaged magnetic well is certainly formed around the separatrix and also local magnetic shear appears due to the toroidal effect. Constant $\oint d\ell/B$ surfaces close themselves, except for those far from the minor axis. Critical lines where $\delta\oint d\ell/B = 0$ exist in the bad region of the torus. Cases when the current in the ring is induced by the time variation of the toroidal field are considered. Minimum B can be formed when the number of the ring exceeds a value which is given by the aspect ratio.

§1. Introduction

A periodic arrangement of inner ring conductors which carry currents encircling the minor axis of a torus produces a minimum B or an averaged minimum B field configuration for plasma confinement.[1) ~ 4)] This field is characterized by the existence of null-field lines as shown in Fig.1. Experiments on a low β plasma confinement showed that a fairly stable plasma is trapped in the field.[5)] Short circuiting currents flowing on the null-field lines were found to reduce the polarization of plasma due to the toroidal drift.[6)] In case of high β plasma produced by toroidal theta pinch, the outward expansion of plasma was well suppressed when the number of rings were enough to form a minimum B.[7)] Besides, usage of many rings makes the connexion length short and depresses the growth rate of resistive ballooning instability.

These inner-ring systems may not be suited for the confinement of fusion plasma, but some auxiliary applications can be considered. One of them is a smooth conversion of toroidal pinch to a normal Tokamak mode. The ion temperature in Caulked Cusp Torus, equipped with 24 inner rings, was inferred to be 200 eV at the first stage of the pinch.[8)] In an electric field for exciting toroidal current is applied in the accompaniment of the decay of the ring currents, a Tokamak plasma with initially high ion temperature may be

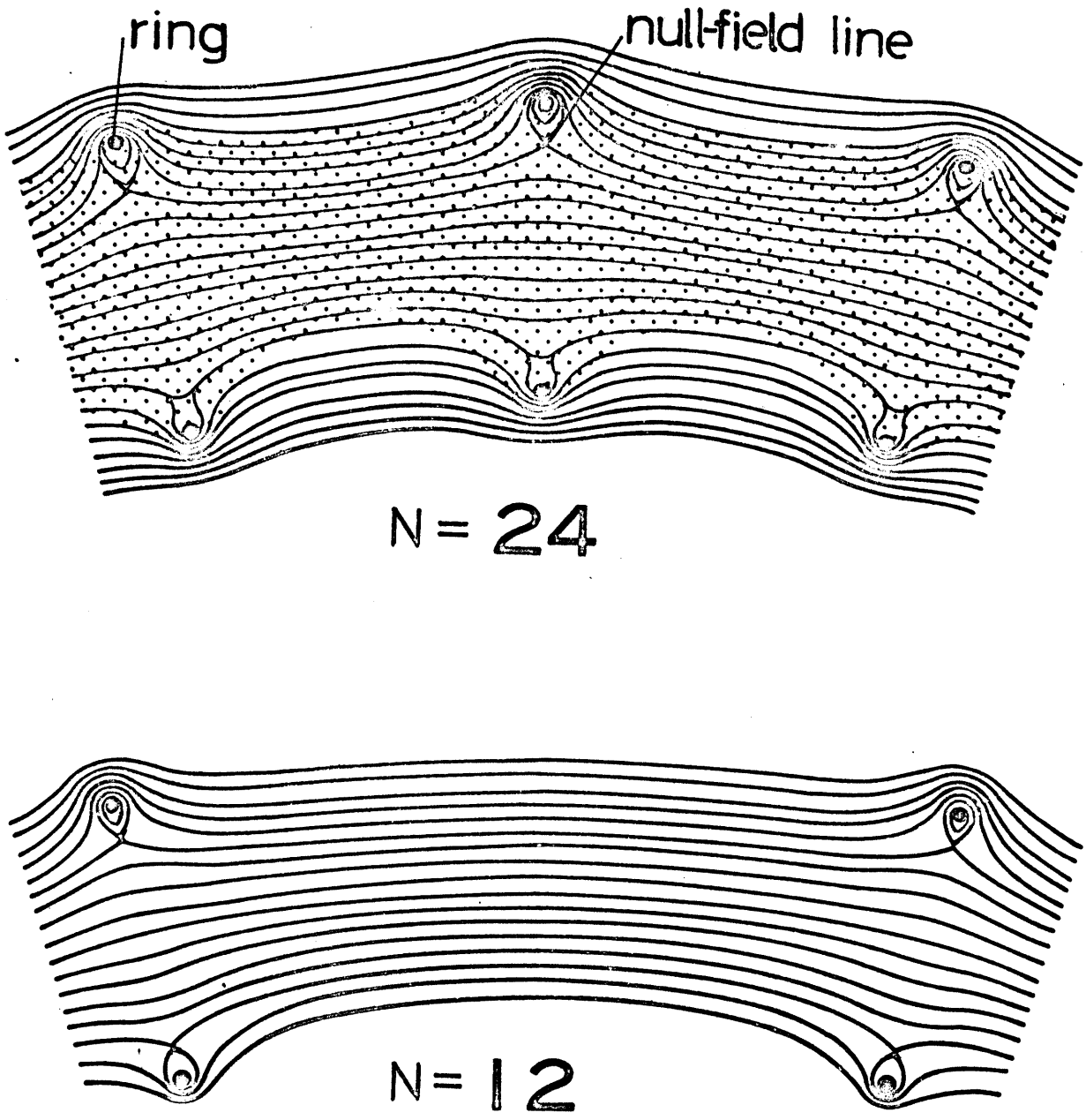

Fig.1 Superposition of a toroidal magnetic field on a magnetic field produced by ring currents which are arranged along the minor axis of a torus. The aspect ratio of the ring is 10, and the currents in the ring conductors are induced by the time variation of the toroidal field. The upper figure is the case that 24 rings are used, and the lower is the case of 12 rings.

realized. Such a field configuration may also be generated by a periodic arrangement of current annulus of plasma. Concepts of Astron[9)10)] and Canted Mirror with relativistic electrons[11)] will be extended to the similar case.

Characteristics of this inner ring system are summarized here, covering the wide range of parameters such as the aspect ratio of the ring radius to the major radius, the amount of the ring current and the used number of the rings. Adding to the results given in ref.(4), the parameters to form the minor-radial minimum B at the midplane of neighbouring rings are examined in the case that ring currents are induced by the time variation of the toroidal field. These calculations offer some foundation for the design of Caulked Cusp Torus II, which is now under planning.

§2. Types and Parameters of the Field Configuration

Here is only considered the case that the magnetic field of the ring current is inverse inside its loop to the toroidal field. The resultant noll-field lines where $B = 0$ change their position as from A to C in Fig.2 with the increase of the ring current. For the linear arrangement of rings, the position of null-field lines is easily given analytically, but the introduction of toroidicity makes it necessary to use a computer method.

The magnetic field is caliculated by assuming the ring current to be a filamentary one, and quasi-toroidal coordinates (r, θ, ϕ) shown in Fig.3 are used. We shall consider the following ring system:

circular filamentary current loops of radius a and magnitude I stay at the planes $\phi = \frac{2\pi}{N} j$; $j = 0, 1, \ldots,$ N-1 and their centres are on the minor axis ($r = 0$) where the major diameter is R.

In order to see the properties of the field, we use the parameters defined as

number of rings : N,

aspect ratio of the ring : $R/a \equiv s$,

and

a normalized ring current : $-(\mu_0 I/2a)/B_0 = \gamma$

where B_0 is the toroidal magnetic induction at $r = 0$ and

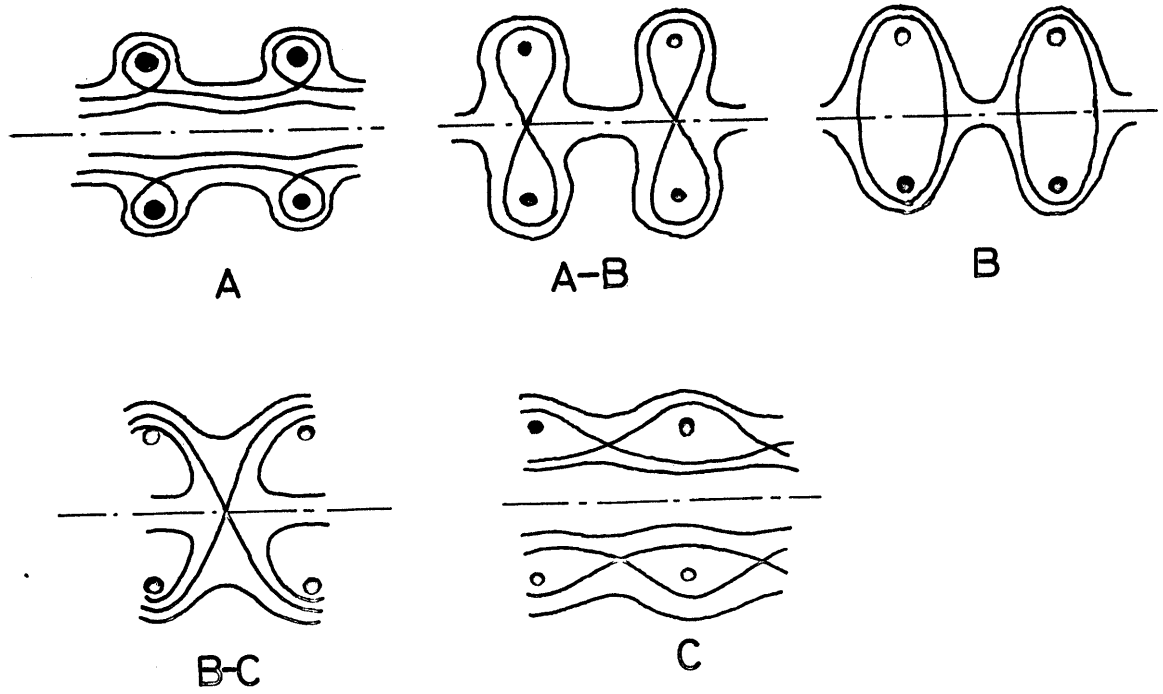

Fig.2 Variation of the field configuration with the increase of the ring current.

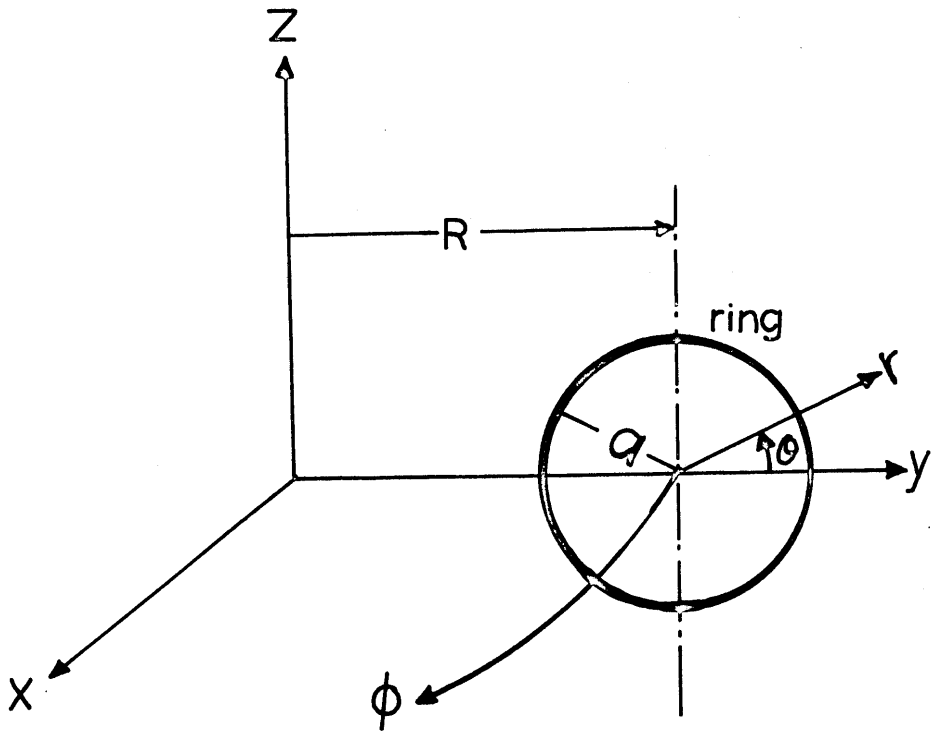

Fig.3 Quasi-toroidal coordinates (r, θ, ϕ).

μ_0 is the magnetic permeability of vacuum. The magnetic induction $\vec{B}$ and r are also normalized such that $\vec{B}^* = \vec{B}/B_0$ and $r^* = r/a$. The magnetic field can be given by above three parameters s, γ and N as expressed in Appendix.

§3. Characteristics of the Field

3.1 Magnetic lines of force and null-field lines

The null-field lines of type A in Fig.2 are approximately elliptic, owing to the toroidicity. The centre of the ellipse shifts toward the major axis of the torus from the centre of the ring. This shift denoted by $\Delta R^* = \Delta R/a$ is not particularly affected by N if γ and s are kept constant. However, keeping γ and N fixed, ΔR^* decreases as s increases, and it becomes less than 10^{-2} for S > 30. Figure 4 shows a typical example of the magnetic induction on a ϕ plane where a ring is located (hereafter the plane is called "ring-plane").

With the increase of γ, the ellipse of the null-field line becomes smaller in size, and finally it degenerates to a point, the position of which is also inside off the minor axis. Then this degeneration breaks again at the larger value of γ (type B in Fig.2). The null-field points go back to the minor axis and shift outwards from the major axis. Such a behaviour of the null-field line or point is shown in Fig.5 for s = 6.366 and N = 8 or 16. In case of type B, there is shown the position only in ϕ^* $(= \phi N/2\pi)$ direction. The transition of the type from A to B occurs at smaller γ for larger N, because the mutual interaction of the magnetic fields produced by ring currents appears appreciably.

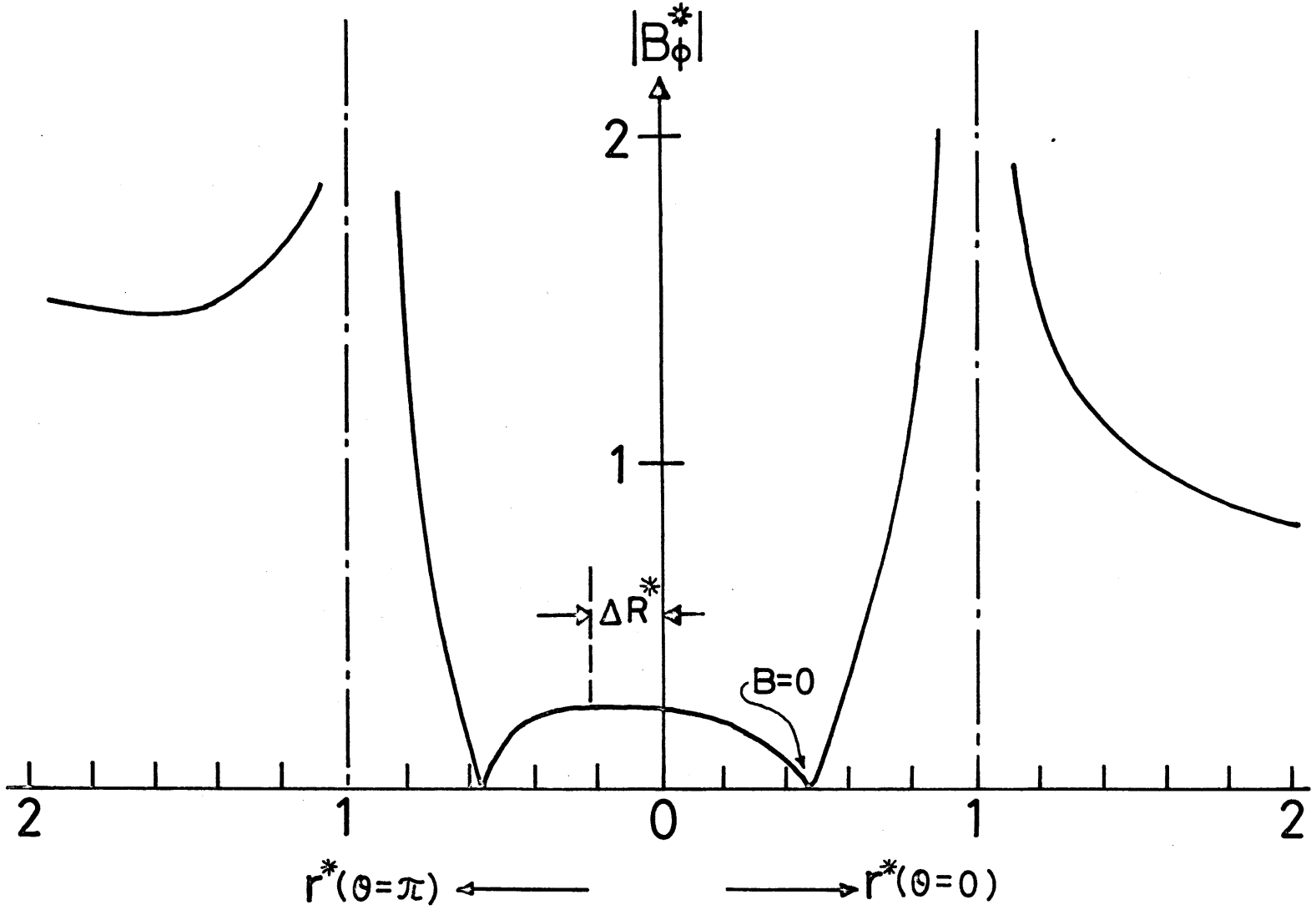

Fig.4 Absolute magnetic induction of type A on the ring plane. N = 8, s = 6.366 and γ = 0.785.

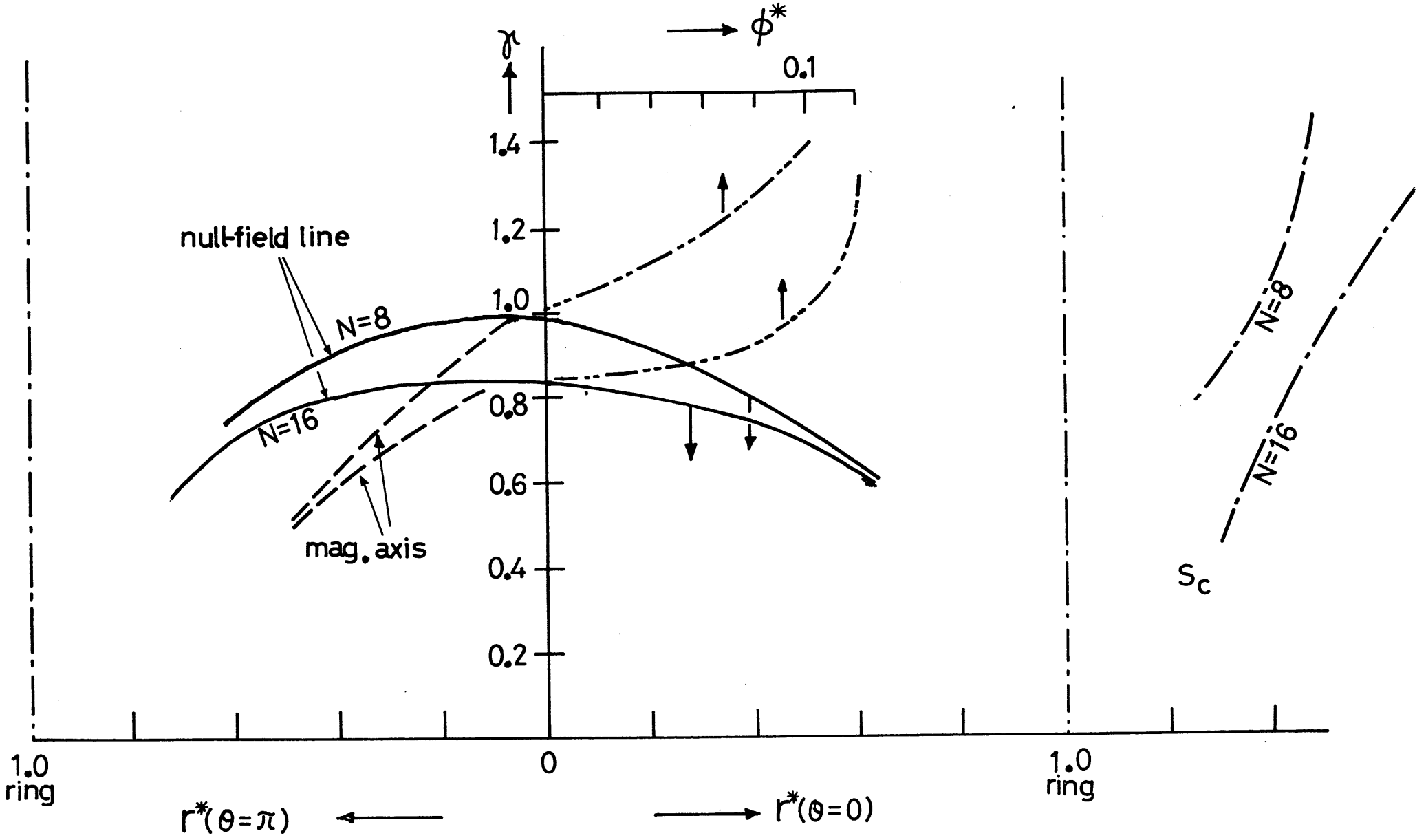

Fig.5 Positions of the null-field line and the critical line S_c on the ring plane as a function of γ for N = 8 and N = 16.

The magnetic lines of force do not stay on a same θ-plane due to the magnetic tension, which arises from the toroidal curvature. Figure 6 shows the azimuthal deviation of a field line which starts from a given point at $\theta = \pi/3$ on the ring plane. We can see there exists weak magnetic shear except for the lines on the meridian plane of the torus. This maximum deviation occurs at the midplane of neighbouring rings for types A and B.

3.2 Integral $U = -\oint d\ell/B$

The outermost line for MHD stability in the limit of low β is determined from the spatial variation of the stability integral $U = -\oint d\ell/B$. The limiting line appears at $dU/dr = 0$. There exists no magnetic surface in this system, since every magnetic field line closes itself with a circuit about the major axis. However, a critical surface can be defined as an ensamble of the limiting lines, which is denoted by S_c. Other two kinds of surfaces are defined: constant U surface S_U and separatrix S_S. The latter is a special one of S_U and formed by the field lines passing through the null-field line. Because of the lack of rotational transform (magnetic surface), the critical surface S_c does not coincide with the constant U surface. The existence of S_S gives an assurance that all S_U inside and just outside S_S are closed.

Hereafter, we use the normalized form given by

$$U^* = \frac{B_0}{a} U$$

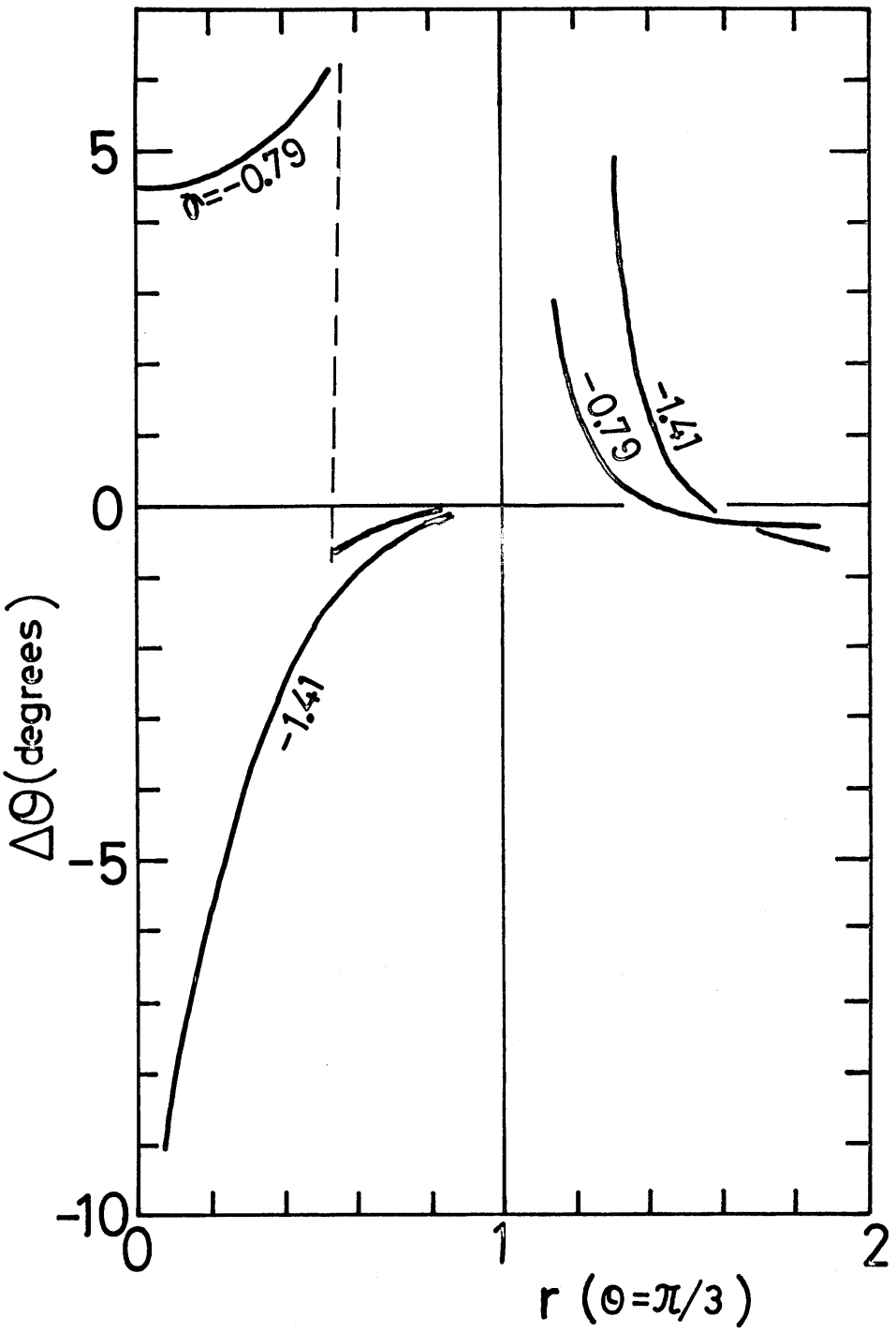

Fig.6 Maximum azimuthal deviation angle $\Delta\theta$ of the magnetic lines of force starting from points at $\theta = \pi/3$ on the ring plane, where $s = 6.366$ and $N = 8$.

Configuration of type A

Figure 7 presents an example of the variation of U^* on the meridian plane ($\theta = 0, \pi$) of the torus in case of type A. The surface S_c exists in only the region $-\frac{\pi}{2} < \theta < \frac{\pi}{2}$. The position where U^* becomes maximum inside S_s shifts toward the major axis from the centre of the ring. We define the field line in this position as "magnetic axis". The shift becomes smaller as the ring current increases, as shown in Fig.5.

Figure 8 shows constant U surfaces S_U in the same condition as in Fig.7. All surfaces inside the separatrix S_s are closed and their centres shift towards the major axis. Outer surfaces near S_s close themselves, but, as going far from S_s, surfaces become open and finaly approach to the shape of cylinder. The critical surface S_c stays only in the bad region of the torus. Thus, the stable region in the limit of low β is determined from the outermost closed U surface which comes into contact with S_c.

In the linear configuration there exist no critical surface and U^* on the magnetic axis is lower than U^* of sufficiently outer lines. However, this is not always true in toroidal configurations. Let U^* on the magnetic axis and on the surface of S_c to be U_A^* and U_c^*, respectively, the ratio

$$\left| U_A^*/U_c^* \right|$$

becomes smaller than unity for small γ. Figure 9 shows the dependence of U_A^*/U_c^* on the parameters γ, N and S. It is

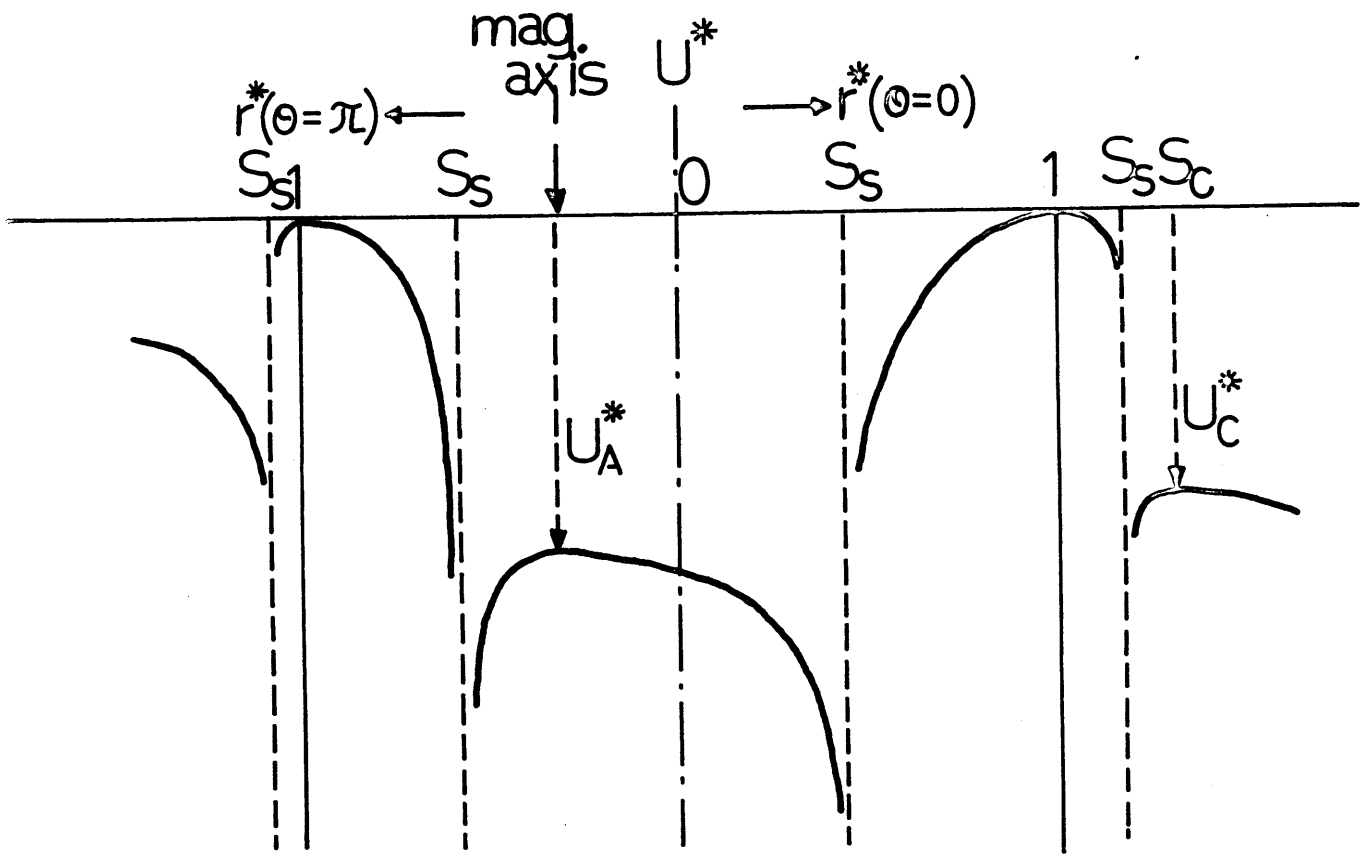

Fig.7 Distribution of the potential U^* on the meridian plane at $\phi = 0$ in case of type A, where $\gamma = 0.785$, $s = 6.366$ and $N = 8$.

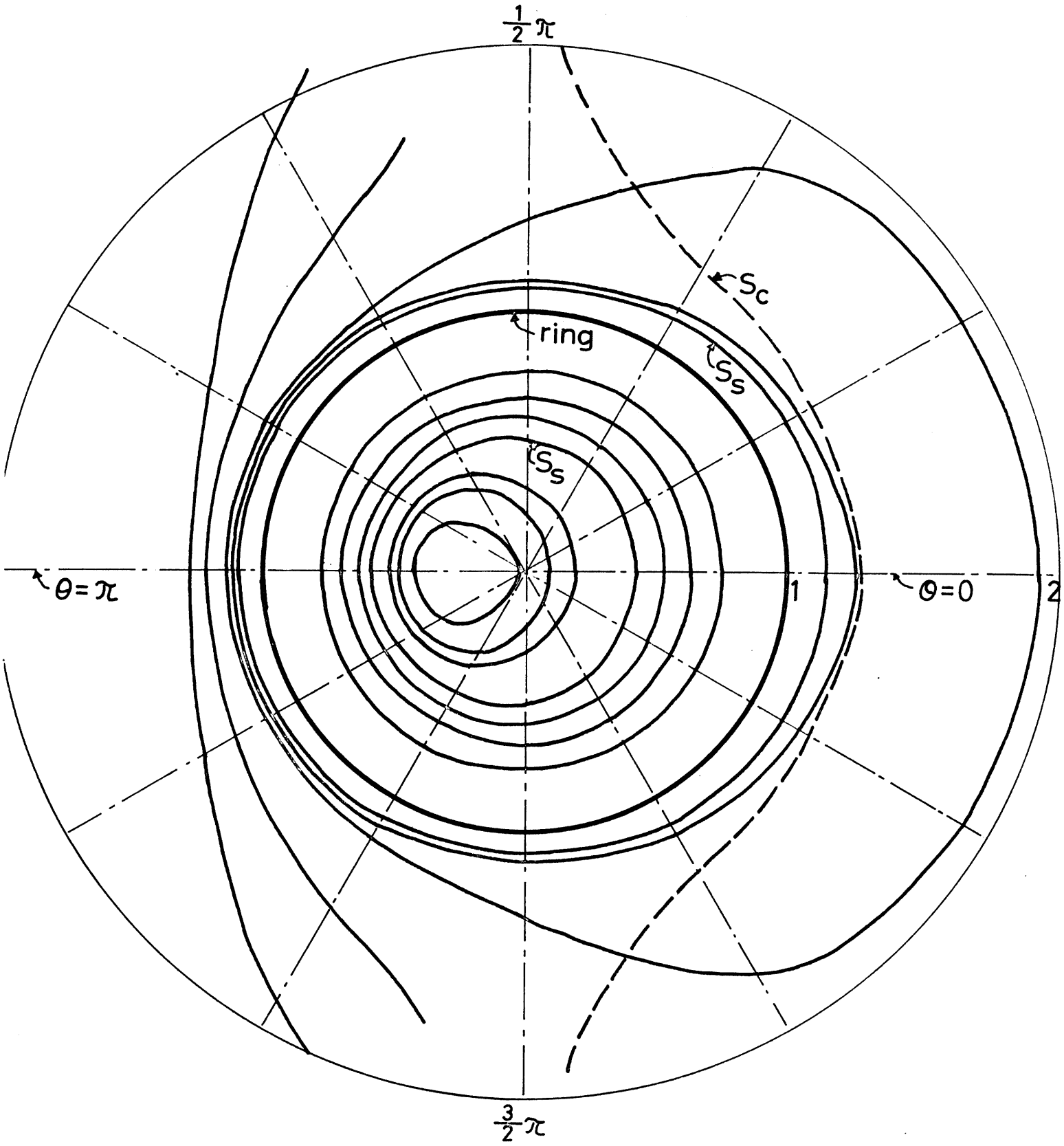

Fig.8 Constant U surfaces S_U of type A configuration, where $\gamma = 0.785$, $s = 6.366$ and $N = 8$. The critical surface S_c and the separatrix S_s are also shown. These surfaces are drawn on the ring plane.

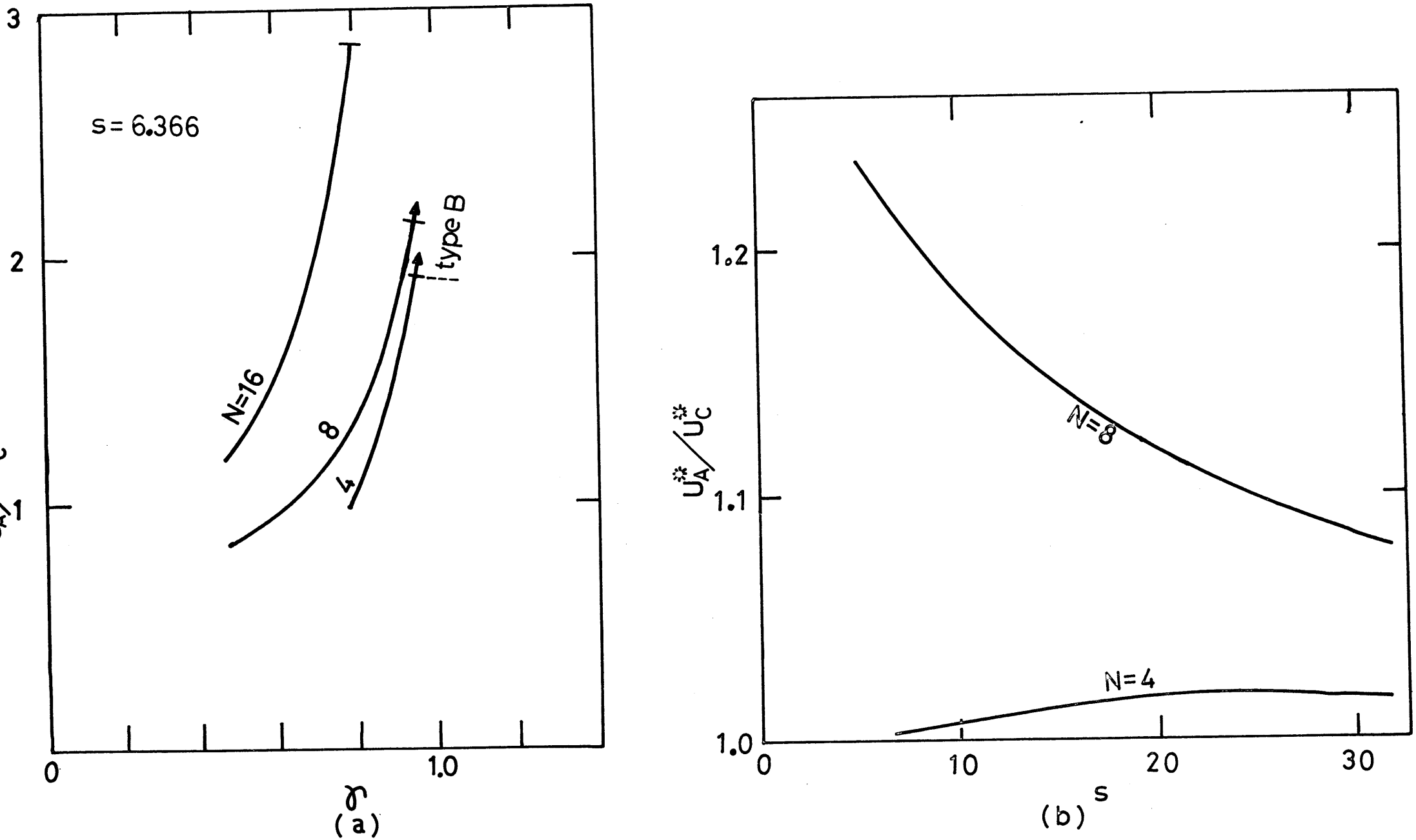

Fig.9 Dependence of $\left|U_A^*/U_C^*\right|$ on γ, N and s.

a) as a function of γ for N = 4, 8 and 16 and s = 6.366.

b) as a function of s for N = 4, 8 and γ = 0.785.

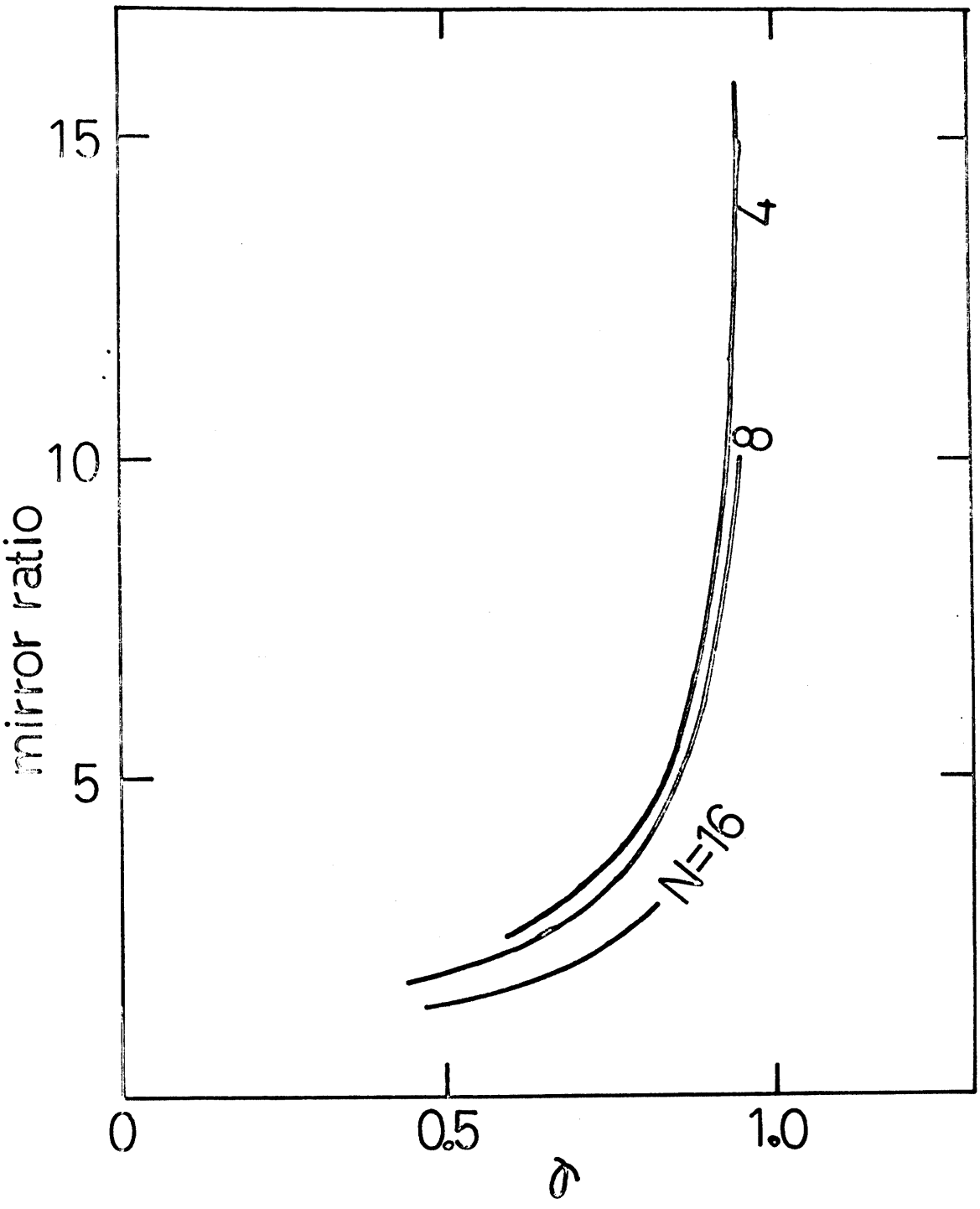

Fig.10 Magnetic mirror ratio along the magnetic axis versus γ for N=4, 8,and 16. s = 6.366.

clear that N is necessary to be large so as to make $\left|U_A^*/U_C^*\right|$ large before the transition of the type from A to B.

The magnetic mirror ratio along the magnetic axis increases with γ and decreases with N, as shown in Fig.10. Thus, in order to have large $\left|U_A^*/U_C^*\right|$ for large γ, the alignment of many rings is necessary.

Configurations of types A-B and B

Figure 11 presents an typical example of S_U surfaces in case of type A-B, where the null-field line is degenerated into a point. The deformation of S_U from a circle is less than in the case of type A. The critical surface S_C deviates far away from the separatrix S_S compared with the case of type A as in Fig.5.

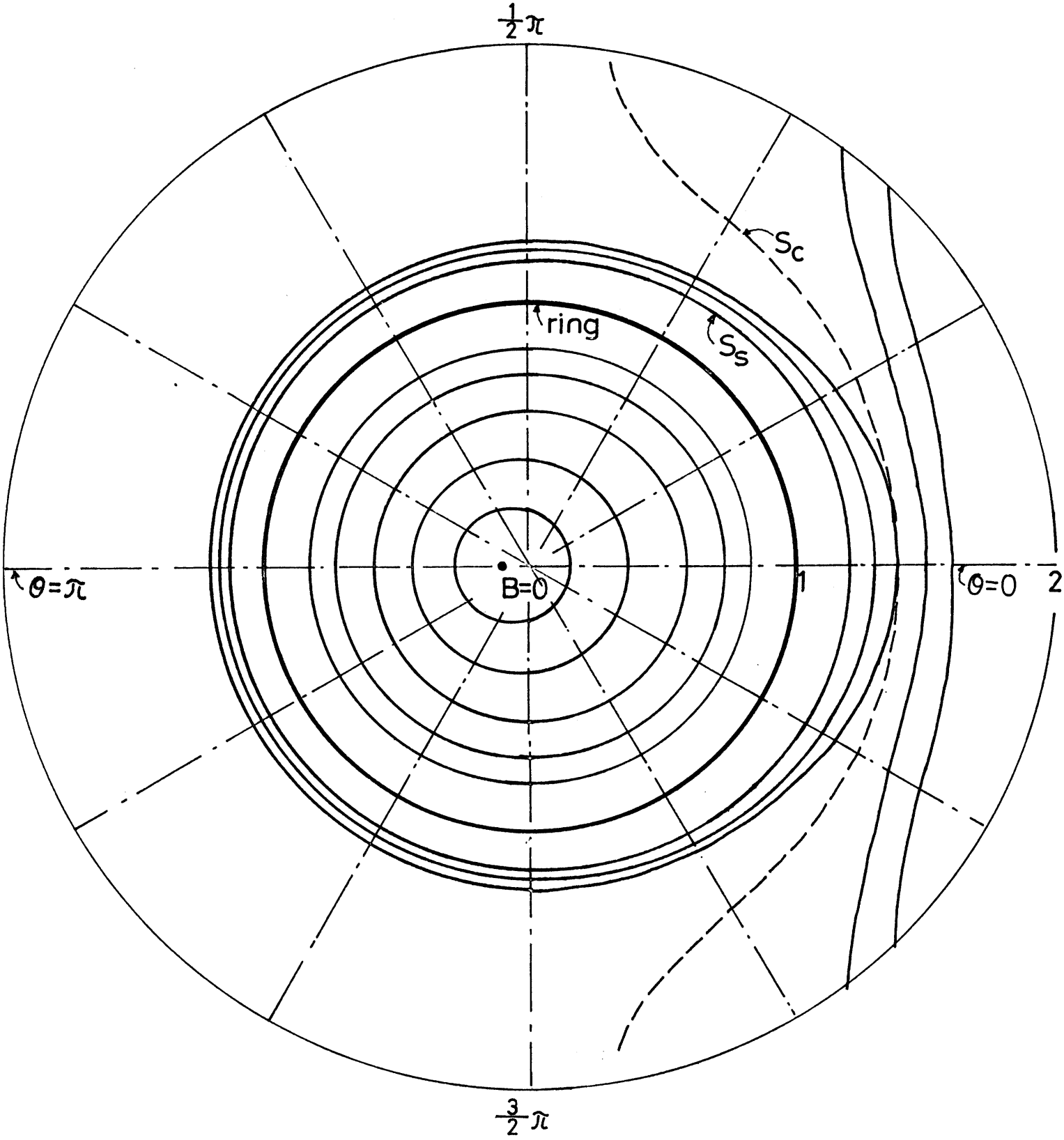

Fig.11 Constant U surfaces and the critical surface S_c in case of type A-B, where $\gamma = 1.1$, $s = 6.366$ and $N = 8$.

§4. Mutual Induction of the Ring Current

The ring current can be induced by the time variation of the toroidal field.[5)7)] This method is much suited for the toroidal theta pinch, since the decay time of ring currents is longer than the time in question and the plasma loss due to current feeders is avoided. Then, the induced current of a ring is estimated from the conservation of magnetic flux in a perfect conductor loop. Using the formula of the self-inductance as

$$L = \mu_0 a \left[\left(1 + \frac{3r_0^2}{16a^2}\right) \log \frac{8a}{r_0} - \frac{r_0^2}{16a^2} - 2 \right] ,$$

$$r_0 = 0.7788\, a_r ,$$

where a_r is the minor radius of the ring, we have

$$\gamma_i = \frac{s}{\beta} \left(1 - \sqrt{1 - \frac{1}{s^2}}\right) ,$$

and $\beta = \frac{\pi L}{\mu_0 a}$. The current parameter γ_i becomes larger as the aspect ratio s decreases.

4.1 Position of null-field lines

Field configurations in this case belong to type A, because $\gamma_i < 1$. The minor-radial position of the null-field line is shown in Fig.12 for different s.

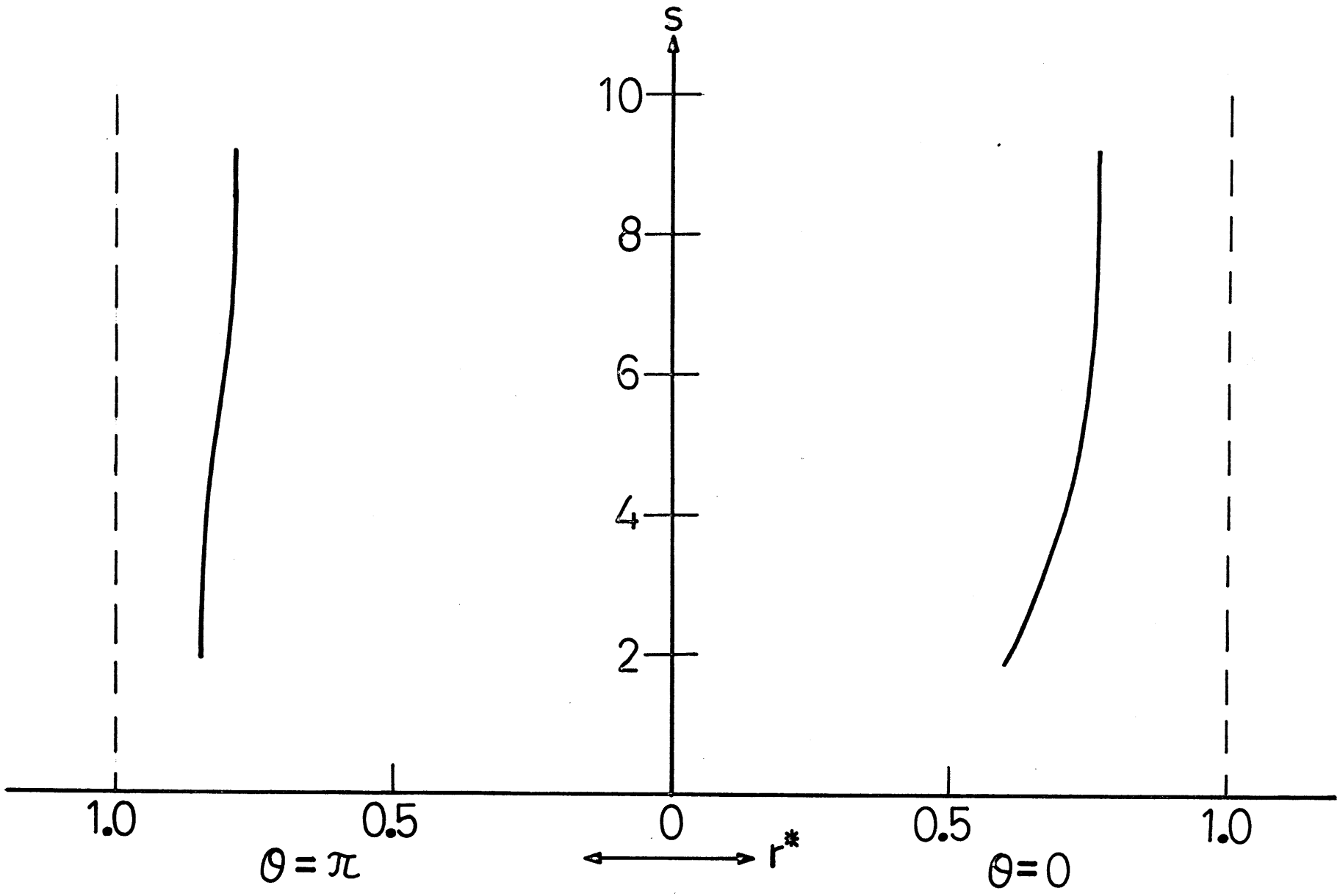

Fig.12 Position of the null-field lines on the meridian plane of the torus at $\phi = 0$ as a function of s. The ring-currents are induced by the toroidal field. The mutual coupling effect among the rings is neglected.

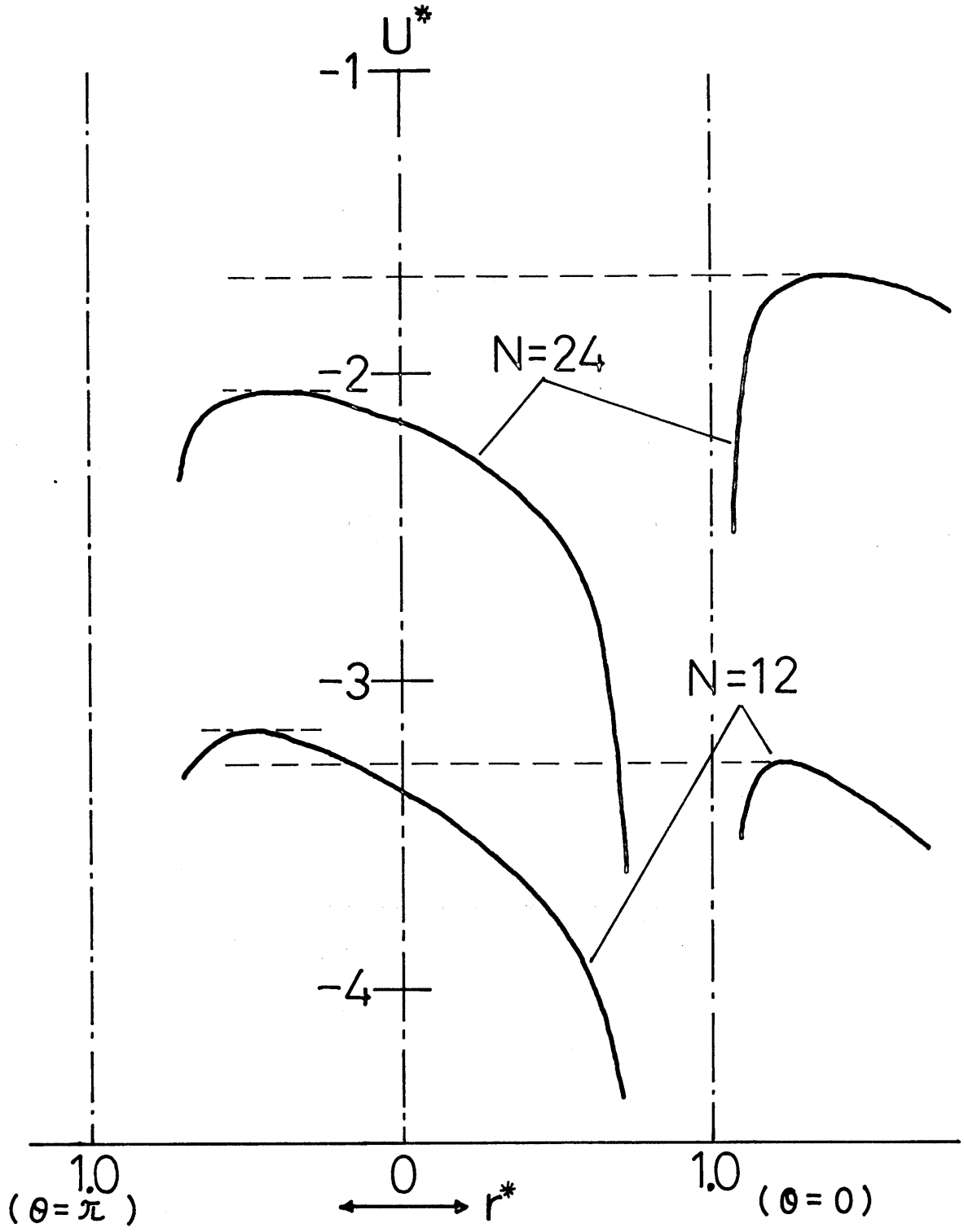

Fig.13 Potentials U^* on the meridian plane at $\phi = 0$ for s = 10 and N = 12, 24. These configurations are used in the experiment of Caulked Cusp Torus.

Fig.14 Bird's eye view of the magnetic pressure in the case that s = 10 and N = 24.

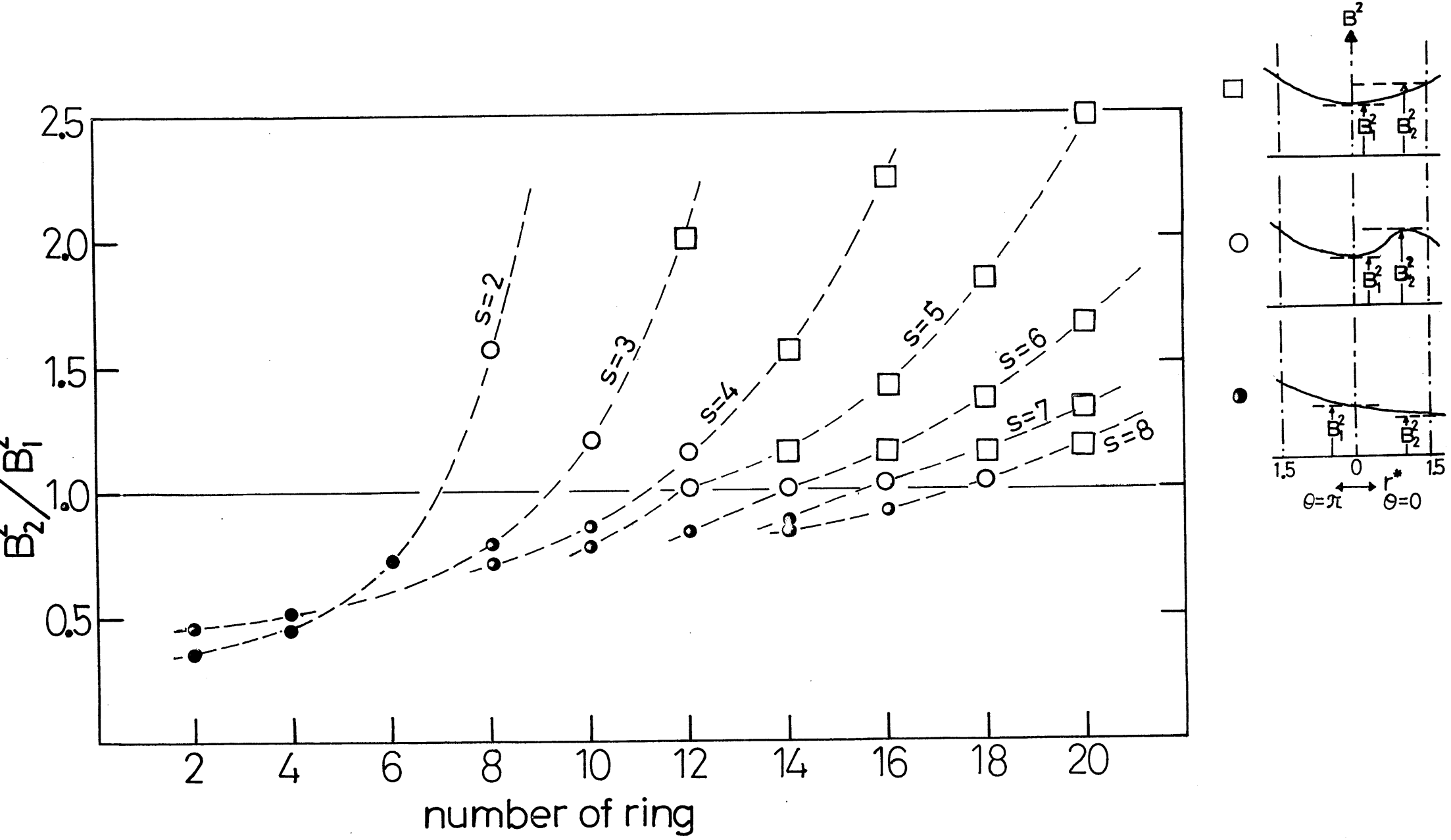

Fig.15 Necessary number of rings to have the well of magnetic pressure for various aspect ratios. The ratio of the magnetic pressure as shown on the right side of the figure are the value at the midplane between neighbouring rings.

4.2 Potnetial U

The potential U changes its value as the parameters s and N vary. Figure 13 gives the dependence of U on N for s = 10, where cases N = 12 and 24 were used in the experiment of Caulked Cusp Torus.[7] Another examples used in the Heliotron-P experiment has been shown in Figs. 7 and 8.

4.3 Condition of min-B in the minor-radial direction

A bird's eye view of the distribution of magnetic pressure is presented in Fig.14 in the case s = 10 and N = 24. We can see there is formed a complete well of magnetic pressure (i.e. minimum B). Experimentally it was shown that this condition is important to suppress the major-radial expansion of high β plasma.[7] If the magnetic pressure increases outward from the minor axis at the midplane between neighbouring rings, a well of minimum B is realized. From Fig.15, we can choose the appropriate parameters to have the well. The well can be formed with smaller number of rings as the aspect ratio becomes smaller.

Acknowledgment

The authors are indepted to Dr. K. Sato for the preparation of figures. They are also grateful to Prefessor H. Yoshimura of Nihon University for encouragement through the work.

It should be noted that Data Processing Centers of Kyoto University and the Institute of Plasma Physics were utilized for the computation.

Appendix

The magnetic field generated by a ring current (B_{Rr}, $B_{R\theta}$, $B_{R\phi}$) is given by

$$B_{Rr} = \cos\theta\cdot\sin\phi\ B_z^0 + \frac{1}{\ell}[\rho\cos\theta\cdot\cos\phi + r\sin^2\theta]B_\rho^0, \qquad \text{(A-1)}$$

$$B_{R\theta} = -\sin\theta\cdot\sin\phi\ B_z^0 + \frac{1}{\ell}[-\rho\sin\theta\cdot\cos\phi + r\sin\theta\cdot\cos\theta]B_\rho^0, \qquad \text{(A-2)}$$

$$B_{R\phi} = \cos\phi\ B_z^0 - \frac{1}{\ell}[\rho\sin\phi]B_\rho^0, \qquad \text{(A-3)}$$

where

$$\rho = R + r\cos\theta \quad , \qquad \text{(A-4)}$$

$$\ell = [\rho^2 + r^2\sin^2\theta]^{1/2} \qquad \text{(A-5)}$$

$$B_\rho^0 = \frac{\mu_0 I(R + r\cos\theta)\sin\phi}{4\pi\sqrt{a}\ \ell^{3/2}}\, k\left[-K(k) + \frac{1 - \frac{k^2}{2}}{1 - k^2}E(k)\right], \qquad \text{(A-6)}$$

$$B_z^0 = \frac{\mu_0 I\sqrt{a}}{4\pi\ell^{3/2}}\, k\left[\frac{\ell}{a}K(k) + \frac{1}{1 - k^2}\left\{\frac{k^2}{2}\left(1 + \frac{\ell}{a}\right) - \frac{\ell}{a}\right\}E(k)\right], \qquad \text{(A-7)}$$

$$k^2 = 4a\ell/\{(a + \ell)^2 + (R + r\cos\theta)^2\sin^2\phi\}, \qquad \text{(A-8)}$$

and K(k) and E(k) are Complete Elliptic Integrals of First and Second kind, respectively.

When N rings are located along the minor axis of the torus at regular intervals, the field by the ring currents at any spatial point (r, θ, ϕ) is

$$\vec{B}_N = \sum_{n=0}^{N-1} \vec{B}_R\left(r,\ \theta,\ \phi - \frac{2\pi}{N}n\right) . \qquad \text{(A-9)}$$

Thus, the magnetic field in our case is expressed by

$$\vec{B} = \vec{B}_N + \frac{B_0}{1 + \frac{r}{R}\cos\theta}\,\vec{e}_\phi \ , \qquad \text{(A-10)}$$

where B_0 is the toroidal magnetic field on the minor axis.

References

1) B. B. Kadomtsev: Plasma Physics and the Problem of Controlled Thermonuclear Reactions (USSR, Academy of Science, 1958) Vol.4, p.417.

2) J. Tuck: Nature 187 (1960) 863.

3) D. S. Wiley: Phys. Fluids 12 (1969) 2434.

4) A. Mohri: Kakuyugo-Kenkyu, circular in Japanese 23 (1969) 231.

5) A. Mohri and M. Inoue: Phys. Letters 35A (1971) 69.

6) H. Oshiyama: J. Phys. Soc. Japan 31 (1971) 1602.

7) T. Uchida, K. Sato, A. Mohri, and R. Akiyama: Plasma Physics and Controlled Nuclear Research (IAEA, Vienna, 1971) Vol.III, p.169.

8) N. Noda, K. Sato, R. Akiyama, N. Inoue and T. Uchida: to be published in Nuclear Fusion.

9) G. Benford, D. L. Book, N. C. Christofilos, T. K. Fowler, V. K. Neil, and L. D. Pearlstein: Plasma Physics and Controlled Nuclear Fusion (IAEA, Vienna, 1968) Vol.I p.981.

10) M. L. Andrews, H. Davitian, H. H. Fleischmann, R. E. Kribel, B. R. Kusse, J. A. Nation, R. Lee, R. V. Lovelace, and R. N. Sudan: Plasma Physics and Controlled Nuclear Fusion (IAEA, Vienna, 1971) Vol.I, p.169.

11) R. A. Dandl, H. O. Easen, P. H. Edmonds, A. C. England, G. E. Guest, C. L. Hedrick, J. T. Hogan, and J. C. Sprott: ibid. Vol.II, p.607.